Footwear-Integrated Force Sensing Resistor Sensors: A Machine Learning Approach for Categorizing Lower Limb Disorders

Hafeez Ur Rehman Siddiqui[a,*], Sunwan Nawaz[a], Muhammad Nauman Saeed[a], Adil Ali Saleem[a], Muhammad Amjad Raza[a], Ali Raza[a], Ahsan Aslam[a], Sandra Dudley[b]

[a]*Institute of Computer Science and Information Technology, Khwaja Fareed University of Engineering and Information Technology, Rahim Yar Khan, 64200, Punjab, Pakistan*
[b]*Bioengineering Research Centre, School of Engineering, London South Bank University, 103 Borough Road, London, SE1 0AA, United Kingdom*

Abstract

Lower limb disorders are a substantial contributor to both disability and lower standards of life. The prevalent disorders affecting the lower limbs include osteoarthritis of the knee, hip, and ankle. The present study focuses on the use of footwear that incorporates force-sensing resistor sensors to classify lower limb disorders affecting the knee, hip, and ankle joints. The research collected data from a sample of 117 participants who wore footwear integrated with force-sensing resistor sensors while walking on a predetermined walkway of 9 meters. Extensive preprocessing and feature extraction techniques were applied to form a structured dataset. Several machine learning classifiers were trained and evaluated. According to the findings, the Random Forest model exhibited the highest level of performance on the balanced dataset with an accuracy rate of 96%, while the Decision Tree model achieved an accuracy rate of 91%. The accuracy scores of the Logistic Regression, Gaus-

*Correspondance: Hafeez@kfueit.edu.pk

Email addresses: `Hafeez@kfueit.edu.pk` (Hafeez Ur Rehman Siddiqui), `compoperator.sunwan@kfueit.edu.pk` (Sunwan Nawaz), `naumansaeed0077@gmail.com` (Muhammad Nauman Saeed), `adilalisaleem@gmail.com` (Adil Ali Saleem), `Ch.amjadraza@gmail.com` (Muhammad Amjad Raza), `ali.raza.scholarly@gmail.com` (Ali Raza), `ahsan.aslam@kfueit.edu.pk` (Ahsan Aslam), `dudleyms@lsbu.ac.uk` (Sandra Dudley)

sian Naive Bayes, and Long Short-Term Memory models were comparatively lower. K-fold cross-validation was also performed to evaluate the models' performance. The results indicate that the integration of force-sensing resistor sensors into footwear, along with the use of machine learning techniques, can accurately categorize lower limb disorders. This offers valuable information for developing customized interventions and treatment plans.

Keywords: Lower limb disorder, Hip, Knee, Ankle, Gait Analysis, Force-sensing resistor sensors, Plantar pressure

1. Introduction

Lower limb disorders are a substantial contributor to both disability and lower standards of life around the globe Fatima (2022); Grimmer et al. (2019). At present, osteoarthritis (OA) stands as the second most prevalent cause of disability Callahan et al. (2021). OA has a global impact, affecting approximately 500 million individuals and it is projected that by the year 2030 it will affect one-third of the global population Carr et al. (2012); Hunter et al. (2020). It is also recognized as one of the prevailing types of arthritis on a global scale, constituting approximately 83% of the overall burden associated with OA Vos et al. (2012). The prevalent disorders affecting the lower limbs include OA of the knee, hip, and ankle Pirani et al. (2019); Leggit et al. (2022). Hip and Knee OA are highly prevalent forms of OA on a global scale, affecting approximately 12% of the global population Dell'Isola et al. (2022); Ferreira et al. (2021). According to Vos et al., the worldwide prevalence of knee osteoarthritis (KOA) exceeds 250 million individuals Vos et al. (2012). Ankle OA is a persistent condition that impacts roughly 1% of the global population. It has an estimated occurrence rate of 30 cases per 100,000 individuals and accounts for approximately 2 to 4% of all patients diagnosed with OA Herrera-Pérez et al. (2022); Goldberg et al. (2012); Herrera-Pérez et al. (2021); Valderrabano et al. (2009). These ailments, typically caused by injury, degenerative illnesses, or biomechanical irregularities, can cause pain, limited motion, and decreased function. For effective treatment planning, individualized rehabilitation, and prevention of additional consequences, prompt and precise classification of these conditions is vital. Clinical tests, subjective patient reports, and diagnostic imaging techniques such as X-rays and magnetic resonance imaging (MRI) have traditionally been utilized as the primary methods for determining the presence and severity of lower limb problems Khalid et al. (2020); Heidari (2011). Even while these techniques are useful, they frequently need the use of specialized apparatus, they take a lot of time Hamza et al. (2023); Devereux et al. (1997), and they may not be able to capture the entire dynamics of joint movement that occur during normal tasks.

Technological progressions have facilitated novel opportunities for the objective and uninterrupted monitoring of biomechanics in the lower extremities in recent times Weygers et al. (2020); Picerno (2017). The integration of force-sensing resistors (FSRs) into footwear is a technology that shows tremendous potential Li et al. (2016); Abdelhady et al. (2019). Flexible and thin sensors known as FSRs are capable of measuring the distribution of pressure and changes in plantar force while walking Malvade et al.. The integration of FSR sensors into common footwear facilitates the acquisition of instantaneous information pertaining to foot pressure, gait patterns, and joint kinetics Malvade et al.; Abdul Razak et al. (2012). The incorporation of FSR sensors into footwear presents numerous benefits for the categorization of lower extremity disorders. Initially, it facilitates the acquisition of extensive datasets in authentic environments, thereby furnishing a broader understanding of individuals' operational aptitudes and difficulties throughout their routine tasks. In addition, it enables extended surveillance, thereby enabling the examination of the advancement of illnesses, reaction to interventions, and the detection of plausible risk elements. Despite the potential advantages of using footwear equipped with FSR sensors to measure plantar pressure, comprehensive study on the classification of lower limb problems is insufficient. So, the objective of the paper is to investigate the viability and efficacy of employing footwear integrated with FSR sensors as a means of categorizing lower limb disorders in the knee, hip, and ankle joints. The aim of this study is to create a classification model that can effectively distinguish between different lower limb disorders by utilizing machine learning techniques in conjunction with sensor data. The model will be based on analyzing gait patterns and foot-loading properties. The findings of this research hold promise in enhancing tailored and empirically supported interventions, ultimately enhancing the management and treatment efficacy for individuals affected with lower limb disorders. The main contributions of this study are:

- A circuit and graphical user interface (GUI) were devised to acquire and record data from FSR sensors, thereby furnishing significant insights into the distribution of foot pressure during locomotion.

- Data was collected from 117 individuals, including both male and female participants, wearing FSR sensor-integrated footwear while walking on a designated walkway at Tehsil Head Quarter (THQ) hospital Sadiqabad.
- The collected matrix data underwent preprocessing techniques to generate mesh images. These images were subsequently subjected to grayscale conversion, wavelet transform, and grey-level co-occurrence matrix analysis.
- Forty-eight features were extracted from the image analysis, providing insights into the composition, spatial arrangements, and configurations of the pressure distribution patterns.
- Several machine learning models, including Random Forest, Decision Tree, Logistic Regression, Gaussian Naive Bayes, and LSTM, were trained and evaluated on the dataset.
- K-fold cross-validation with 10 folds was employed to assess model performance.

The following sections of this article will explore the literature review and methodology. Furthermore, we will have discussions on the results.

2. Literature Review

Joint abnormalities have a substantial impact on the way humans walk, resulting in functional limitations and a diminished quality of life. Therefore, it is essential to promptly identify and accurately classify these abnormalities to ensure effective treatment and rehabilitation. In recent times, there has been an increasing interest in harnessing the potential of machine learning and deep learning techniques to analyze gait data and automatically classify joint abnormalities. The study Kotti et al. (2017) focuses on the development of a computer system for the purpose of detecting knee osteoarthritis in an automated manner. The research gathered walking data from a sample of 47 individuals diagnosed with knee osteoarthritis and 47 individuals without the condition, with the aim of maintaining an equitable representation of both groups. The participants walked on a pathway that was outfitted with force plates that incorporated piezoelectric sensors capable of measuring three-dimensional forces. Several parameters pertaining to ground reaction forces, including mean value, push-off time, and slope, were extracted. The parameters were mapped to the degree of knee osteoarthritis using rule induction through the utilization of random forest regressors. In order to improve the generalizability of the results, a protocol that is independent of the subjects was utilized. The accuracy of the system was evaluated using a 5-fold cross-validation technique, resulting in a mean accuracy of 72.61% with a standard deviation of 4.24%.

The study Cui et al. attempts to precisely evaluate and diagnose gait abnormalities in patients with osteoarthritis by employing a supervised classifier and an RGB-D camera. The research has established a framework for assessing gait, gathered joint data from both healthy individuals and patients, and derived a total of fourteen quantitative parameters related to gait. The investigation incorporates information obtained from a sample of 19 individuals diagnosed with osteoarthritis and 19 individuals who do not exhibit any symptoms of the condition. The study's findings indicate that there are notable variations in gait parameters between individuals diagnosed with osteoarthritis OA and those who are considered healthy, as determined through statistical analysis and experimental results. The supervised support vector machine (SVM) classifier that was developed has demonstrated a noteworthy mean accuracy of 97% in the classification of gait abnormalities. The Verlekar et al. (2018) introduces a system designed for the automated identification and categorization of gait abnormalities, utilizing a solitary 2D video camera. The system employs biomechanical gait characteristics that are derived from the video data, encompassing measurements pertaining to both the feet and the body. The research employed a repository of binary silhouettes representing ten subjects who were emulating eight distinct types of gait impairments. The gait cycles were captured in a LABCOM studio, with multiple sequences recorded at a frame rate of 30 frames per second. The type of impairment was annotated manually, representing the ground truth. The classification task was accomplished through the utilization of a SVM, which yielded a noteworthy accuracy rate of 98.8%.

A system for acquiring and analyzing gait has been developed by Chen et al. (2020) with the aim of offering an affordable and user-friendly solution for the quantitative recording and functional identification of patients with osteoarthritis. Initially, a clinical-oriented automatic gait acquisition platform is devised utilizing an RGB-D camera and bespoke gait data recording software. Furthermore, an assessment is conducted on the efficacy of the gait acquisition platform's operational area for clinical purposes through a comparative analysis with the ground-truth data obtained from infrared optical trackers. Subsequently, the obtained gait data is subjected to analysis utilizing a unique hybrid prediction model in order to evaluate gait abnormalities in a quantitative and objective manner. The hybrid model incorporates both manually extracted features and automatically extracted features from a Long Short-Term Memory (LSTM) network in the analysis of gait data. Empirical findings obtained from actual patients indicate that the suggested gait analysis framework has the capacity to accurately forecast gait anomalies in a quantitative manner, achieving a high level of accuracy at 98.77%. The Jun et al. (2021) introduces an innovative approach to categorize anomalous gait patterns through the utilization of deep learning (DL) methodologies and by integrating 3D skeletal information acquired through the employment of a depth camera with plantar foot pressure measurements. A collection of gait patterns was obtained, consisting of a single instance of normal gait and five instances of pathological gait. The pathological gaits included antalgic, lurching, steppage, stiff-legged, and Trendelenburg. A hybrid model that integrates multiple modes of data was developed to classify various gaits. In order to proficiently derive characteristics from the sequential skeleton and average foot pressure data, encoding layers based on recurrent neural network (RNN) and convolutional neural network (CNN) were employed, correspondingly. The concatenated output features obtained from said layers were subsequently fed into fully connected layers to facilitate classification. The classification accuracies of the models that relied exclusively on pressure or skeleton data were 68.82% and 93.40% respectively. The study findings indicate that the implementation of the multimodal hybrid model resulted in enhanced performance, as evidenced by a 95.66% accuracy rate. In order to optimize the performance, a three-step training approach was implemented to refine the hybrid model, resulting in a final accuracy rate of 97.60

The objective of the Kwon et al. (2020) was to devise an automated categorization framework for knee osteoarthritis (KOA), which relied on radiographic imaging and gait analysis data and was based on the Kallgren-Lawrence (KL) grading system. The study utilized a support vector machine to classify knee osteoarthritis based on gait features and radiographic image features extracted from a deep learning network (Inception-ResNet-v2). The results showed a strong association between gait features and the radiological severity of knee osteoarthritis. The AUC values of the receiver operating characteristic curve for KL Grades 0-4 were 0.93, 0.82, 0.83, 0.88, and 0.97, in that order. The evaluation metrics of the model included sensitivity, precision, and F1-score, which were reported as 0.70, 0.76, and 0.71, respectively. The objective of Chopra and Crevoisier (2019) was to evaluate the degree of gait symmetry among individuals affected with unilateral ankle osteoarthrosis (AOA) and to identify potential factors contributing to gait asymmetry subsequent to ankle surgical interventions. The study employed 3-D inertial sensors and pressure insoles to assess a sample of 20 individuals, comprising of 10 healthy controls and 10 patients with age-related osteoarthritis (AOA). The researchers conducted an analysis of 46 distinct parameters related to gait and examined the relative motions of sub-regions of the foot. The findings indicate notable dissimilarities between the control group and individuals with AOA in 23 variables on the impacted side and 20 variables on the non-impacted side. Differences were observed in 14 parameters, primarily in the toe region, when conducting bilateral comparisons among patients with AOA. The investigation additionally recognized inconsistencies in forefoot relative motion during gait.

The study Slijepcevic et al. (2017) puts forth a comprehensive investigation on the automated categorization of functional gait disorders (GDs) through the utilizations of ground reaction force (GRF) measurements. The study aims to achieve two primary objectives. Firstly, it seeks to investigate the efficacy of contemporary ground GRF parameterization techniques in discerning functional GDs. Secondly, it aims to establish a fundamental reference point for the automated classification of functional GDs through the utilization of a comprehensive dataset. The study employed a dataset comprising of GRF measurements obtained from 279 patients diagnosed with GDs, alongside data from 161 healthy individuals who were included as controls. The patients were classified into four distinct categories based on the functional impairments that were associated with the hip, knee, ankle, and calcaneus. This categorization was performed manually. The study investigated several parameterization techniques, namely GRF parameters, global principal component analysis (PCA) based representations, and a combined representation utilizing PCA on GRF parameters. Linear discriminant analysis was employed to assess the discriminative ability of each parameterization. Two classification experiments were carried out based on the analysis. The primary objective of the initial study was to distinguish between normal and abnormal walking patterns, specifically comparing the healthy group to the GD group. The subsequent trial encompassed multiclass classification, discerning between the normal gait and the four distinct classes of Gait Deviation. The main aim of the study conducted by Shuzan et al. (2023) was to examine the utilization of gait analysis, particularly focusing on GRF, for the purpose of classifying gait disorders. The researchers utilized two databases, specifically GaitRec and Gutenberg, which contained data from individuals who had been diagnosed with gait disorders, as well as a control group of individuals without such disorders, who were considered to be in good health. The gait disorders encompassed abnormalities in the hip, knee, ankle, and calcaneus. The GRF signals underwent preprocessing, and a variety of feature extraction algorithms were used. Furthermore, the utilization of feature selection algorithms was employed to identify the most relevant features by eliminating highly correlated ones. The K-nearest neighbor (KNN) model consistently exhibited higher levels of accuracy in comparison to the alternative machine learning techniques that were assessed. Four experimental schemes were conducted to classify gait disorders into binary, three-class, four-class, and five-class categories. Additionally, a comparative analysis was undertaken to evaluate the performance of vertical GRF and three-dimensional GRF. The results of this analysis demonstrated that the latter displayed improved overall performance.

The researchers developed an automated and precise diagnostic system for knee osteoarthritis (KOA) Zeng et al. (2023). The classification potential of different dynamical features extracted from gait kinematic signals was assessed in order to accomplish this task. The research conducted by the authors Zeng et al. (2023) introduced a comprehensive framework that aims to extract various features. This framework encompasses a wide range of dynamical features obtained through the application of recurrence quantification analysis (RQA), fuzzy entropy, and statistical analysis. The aforementioned characteristics encompass the recurrence rate, determinism, and entropy. In this study, a range of shallow classifiers including SVM, KNN, Naïve Bayes, decision tree (DT), and ensemble learning based Adaboost (ELA) classifiers were assessed to perform discriminant analysis on different dynamical gait features. The dataset consisted of tibiofemoral joint angle and translation waveforms collected from a group of 26 individuals diagnosed with KOA and 26 age-matched asymptomatic healthy individuals who served as the control group. The assessment of classification accuracy was performed using two-fold and leave-one-subject-out cross-validation methodologies. The SVM classifier exhibited the highest degree of accuracy, attaining a 92.31% accuracy rate in differentiating between patients with KOA and healthy individuals. Furthermore, it achieved a perfect accuracy rate of 100% in accurately distinguishing between the two groups. A novel approach for computer-aided diagnosis (CADx) utilizing Deep Siamese convolutional neural networks and a fine-tuned ResNet-34 architecture was presented by Cueva et al. (2022). This aims to detect OA lesions in both knees simultaneously, following the KL scale. The training phase utilized a publicly available dataset, while the validation phase was conducted using a privately held dataset. Transfer learning was employed to address the challenges associated with imbalanced datasets. The average multi-class accuracy of the model results is 61%, indicating superior performance in classifying classes KL-0, KL-3, and KL-4 compared to KL-1 and KL-2.

The primary goal of these studies is to investigate various aspects of gait analysis, the classification of gait abnormalities, and the identification of specific joint-related conditions, such as OA and functional gait disorders GDs. These studies utilize diverse types of data, including gait parameters, measurements of GRF, signals of gait kinematics, radiographic imaging, and video data. Various methodologies are employed, such as Machine Learning (ML), DL, RF, SVM, and KNN algorithms, in order to attain accurate classification and diagnosis. In contrast, the primary objective of the current study presented in this manuscript is to examine the identification of lower limb disorders by utilizing gait data acquired through the implementation of FSR sensors. The primary aim of this research is to establish a comprehensive theoretical structure for the recognition and classification of various forms of lower limb disorders, including conditions affecting the knee, ankle, and hip.

3. Proposed Methodology

The analysis of gait is an extremely important component in the process of diagnosing injuries to the lower limbs, particularly those that involve the hip, knee, and ankle joints. The methodology being proposed utilizes data obtained from force-sensing resistor (FSR) sensors for the purpose of categorizing injuries that occur in the knee, hip, and ankle joints. The diagram presented in Figure 1 illustrates the methodology diagram, which offers a comprehensive outline of the various components and flow of the proposed system. The initial phase encompasses the acquisition of raw data from the participants utilizing FSR sensors throughout the complete gait cycle. The gait cycle refers to the sequential patterns of motion exhibited by an individual's lower extremities during the act of walking. The raw data comprises uninterrupted measurements of pressure and force exerted by feet over a period of time, offering significant insights into the individual's gait patterns and characteristics. This data is subsequently stored in a cloud to facilitate subsequent analysis and enhance its accessibility. During the subsequent phase, the raw data that has been collected underwent pre-processing in order to eliminate any undesired noise or artifacts that may have been captured during the data collection process. After the data has undergone the process of cleaning and preparation, appropriate features are derived from the FSR sensor data. The process of feature extraction plays a vital role in reducing the complexity of the data while preserving pertinent information that is pertinent to the diagnosis of disorders. Machine learning (ML) models are used in the third stage to classify FSR sensor data based on derived features. ML models are trained on labeled datasets, in which each data instance is associated with a particular class (e.g., hip, knee and ankle disorder). During the training phase, the ML algorithms discover patterns and connections between the retrieved features and the labels. In the last stage, the efficacy of the ML models is tested using a test dataset that the models have not seen during training. Accuracy, precision, recall and F1 score are the metrics used for assessment. These metrics offer valuable insights regarding the efficacy of the models in accurately classifying disorders.

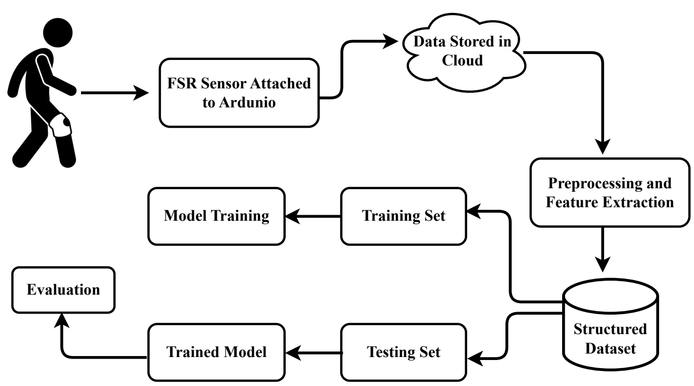

Figure 1: Proposed methodology diagram.

3.1. Circuit and Graphical user interface designing

A circuit and graphical user interface (GUI) as shown in Figure 2 (a) and 2 (b) respectively have been developed to capture and log data from FSR sensors. To simplify the system, a subset of five pressure areas on the human foot has been chosen based on the findings of reference Malvade et al.;

Siddiqui (2016); Wertsch et al. (1992); Rana; Shu et al. (2010). The results of the studies Siddiqui (2016); Wertsch et al. (1992); Rana; Shu et al. (2010) indicated that the regions of greatest pressure on the plantar surface were observed at the heel, the first metatarsal head, the third metatarsal head, the fifth metatarsal head, and the big toe that can be observed in Figure 2 (a). The captured data provides valuable insights into the distribution of pressure during locomotion. Arduino Arduino (2018); Ben, a popular microcontroller platform, is used in this manuscript due to its widespread availability, ease of use, and interoperability with a large range of sensors and actuators. The FSR sensors utilized in this investigation operate within the voltage range of 5V, which is in accordance with the standard voltage supply supported by Arduino FSR. In addition, the FSR sensors offer analog output, making them compatible for direct integration with the analog input pins of the Arduino. This allows the Arduino's analog input pins to directly read force or pressure values from the FSR sensors. Arduino interprets sensor data by converting resistance changes into meaningful force or pressure readings. The GUI, developed using Python as shown in Figure 2 (b), plays a crucial role in controlling the data logging process.

The GUI includes two buttons: "Start" and "Stop." When the "Start" button is pressed, it triggers the data logging process. However, it is important to note that although Arduino continuously sends data to the computer via the Zigbee module, the actual logging of data to the computer begins only when the "Start" button is pressed. This feature provides greater control over the data collection process, allowing for selective logging during specific periods of interest i.e., walking. Once the data logging is initiated, the FSR sensors capture pressure points as the person walks. The collected data is then logged in separate files on the computer, with each foot's data recorded individually. This simultaneous data logging and analysis from both feet offer comprehensive insights into the pressure distribution during locomotion. To conclude the data logging session, the "Stop" button in the GUI is pressed. This action signals the computer to stop the data logging process. The utilization of Zigbee communication is a key component of this system. Zigbee enables wireless connectivity Xbee; Brown et al. (2017) between the computer and the Arduino microcontroller. Wireless sensor networks (WSNs) play a crucial role in the Internet of Things (IoT) landscape. They consist of distributed nodes interconnected wirelessly with various sensors, such as pollution, temperature, and light sensors. These networks enable non-intrusive communication systems that can be deployed in diverse environments, from homes to large commercial settings Brown et al. (2017); Kabir et al. (2014). The edge nodes in WSNs are compact and equipped with microprocessors, memory, and transceivers. In our work, we have designed a wireless network based on XBee, utilizing the ZigBee protocol Xbee; Brown et al. (2017) , and integrated it with the FSR setup to transmit foot pressure data to a remote server for storage in a CSV file. XBee modules adhere to the IEEE 802.15.4 standard, making them efficient in terms of power consumption, maintenance, and self-organization Brown et al. (2017); Kabir et al. (2014). Within the XBee network, a single coordinator device takes charge of network formation, address handling, and network management. The other XBees connected to the coordinator are known as routers or end devices. They can join the existing network, send information, and route information in the case of routers Faludi (2010)."This wireless communication capability enhances the system's flexibility and convenience, eliminating the need for physical connections and allowing for seamless data transmission. For the

(a) (b)

Figure 2: (a) Schematic diagram of the proposed system. (b) GUI designed for the system.

successful data collection, the designed setup is shown in Figure 3.

3.2. Data Collection

To ensure adherence to ethical guidelines, the study received approval from the Khwaja Fareed University of Engineering and Technology (KFUEIT) ethics committee. The committee thoroughly evaluated the study's ethical implications, taking into account the principles outlined in the Helsinki Declaration. By obtaining ethical approval, the study demonstrated its com-

Figure 3: Designed setup for data collection.

mitment to upholding the welfare, rights, and privacy of the participants throughout the research process. Data was collected at the tehsil headquarter hospital Sadiqabad. The data was gathered from 117 individuals aged between 40 and 60 years, comprising both male and female participants. Table 1 presents information on the number of subjects and their respective genders.

Table 1: Subject distribution among different classes.

	Ankle		Knee		Hip	
Gender	Male	Female	Male	Female	Male	Female
No. Of Subjects	21	15	39	20	7	15
Total	36		59		22	

The subjects wore footwear that was outfitted with FSR sensors that were integrated into the soles. The sensors were strategically positioned to record the manner in which the participants' feet applied force while walking. During the experiment, the subjects walked a 9-meter pathway as shown in Figure 4. while the FSR integrated into their footwear captured and quantified the magnitude of the pressure applied to the soles of their feet with each stride. The pressure distribution patterns were captured by the sensors. Each participant is requested to walk 10 times, interspersed with rest periods, to ensure patient comfort and convenience during the study. This approach facilitated the acquisition of reliable data for further processing, feature extraction, and subsequent analysis using the FSR sensor technology.

Figure 4: Subject walking while wearing the designed footwear.

The plantar pressure snippets captured during the walk, as depicted in Figure 5, offer significant insights. The observations reveal that the subject exerts the highest pressure on the toe of their left foot. Furthermore, there is noticeable pressure exerted on the metatarsal regions 1, 2, and 3 of the mentioned foot. Meanwhile, the heel of the left foot is observed to be in the air during this moment. On the contrary, the distribution of plantar pressure on the right foot exhibits a distinct pattern. The right foot's heel maintains contact with the ground while the toe is elevated from the surface. This indicates a distinct weight distribution and movement pattern between the left and right feet during the walking sequence.

Figure 6 displays the mesh image of gait signature of a subject based on ten walking instances. The graph depicts the frequency of transmitted data on the Y-axis, reflecting the intensity of foot pressure events. The X-axis represents different foot pressure regions for the left and right foot. This visualization allows for the identification of patterns and abnormalities in pressure distribution throughout the gait cycle.

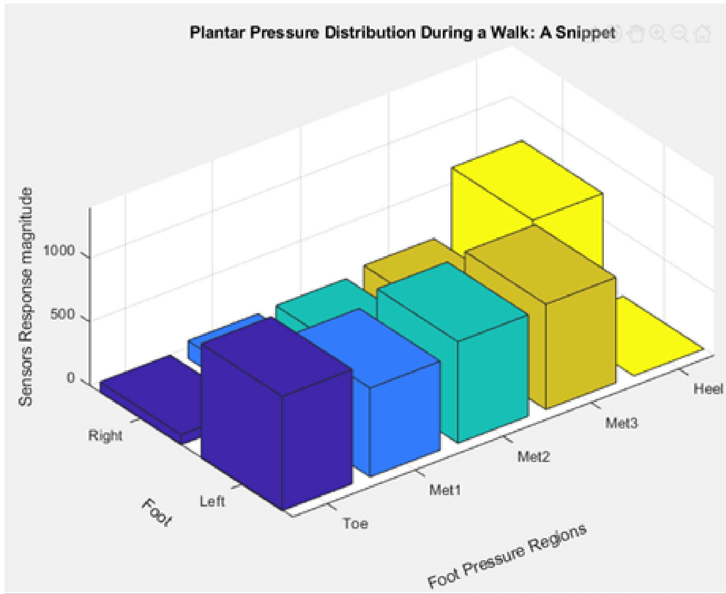

Figure 5: Snippets of plantar pressure during walk.

3.3. Preprocessing and Feature Extraction

The process of preprocessing is of utmost importance in enabling the understanding and assessment of the gathered data. In this study, the preprocessing step involved converting the collected matrix data into mesh images as shown in Figure 6. Subsequently, the images were stored in distinct directories denoted as "knee," "ankle," and "hip," which corresponded to the specific joints under examination. In order to improve the analysis, the mesh images underwent a conversion to greyscale, followed by the application of a single level 2D discrete wavelet transform. The conversion led to the extraction of four distinct groups of coefficients, namely the approximation (LL), horizontal (LH), vertical (HL), and diagonal (HH) detail coefficients. The coefficients offer significant insights pertaining to the distinct frequency components and directional characteristics exhibited by the images. A grey-level co-occurrence matrix (GLCM) was carried out for each decomposed matrix, given that the images were grayscale. The GLCM matrices were generated with a dimension of 256 rows and 256 columns and obtained at three distinct angles, namely 0 degrees, 45 degrees, and 135 degrees.

The matrix comprises individual elements, denoted as C (i, j), which correspond to the frequency of a pixel with a value of i followed by a neighboring

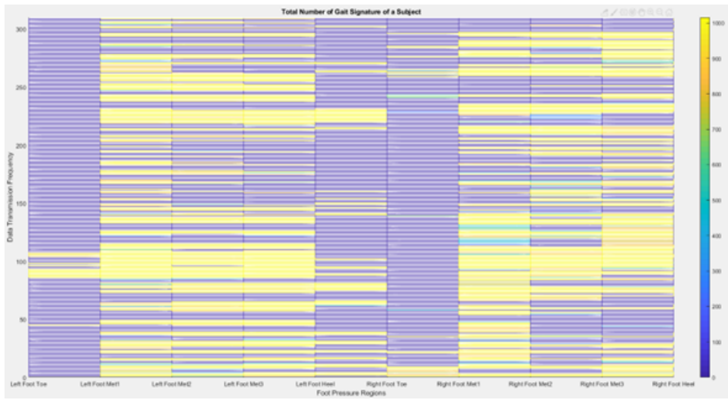

Figure 6: Gait signature of a subject for 10 times walks.

pixel with a value of j in the rightward direction. The procedure was repeatedly executed on each constituent of the GLCM matrix. Following that, a normalization technique was used to limit the values to a predetermined range, typically 0 to 1. Furthermore, statistical characteristics were obtained from the normalized GLCM. The statistical characteristics encompassed various metrics, such as energy, contrast, dissimilarity, and homogeneity. The features yielded significant observations regarding the composition, spatial arrangements, and configurations inherent in the visual representations. A total of forty-eight features were obtained by combining the extracted features from each decomposed matrix. The features are stored in a CSV file, accompanied by their corresponding labels for further analysis. Several suitable ML classifiers were trained results are shown in results section.

3.4. Exploratory Data Analysis

Exploratory Data Analysis (EDA) is a crucial step in conducting a comprehensive and insightful data analysis. During EDA, data is examined to uncover patterns, relationships, and anomalies that may exist within the dataset. This involves the use of various statistical techniques and data visualization methods to gain valuable insights. The statistical analysis of the dataset features is illustrated in Figure 7. This analysis encompasses all the dataset features. We evaluated the count, mean, standard deviation (std), minimum (min), 25th percentile, 50th percentile, 75th percentile, and maximum (max) values for each feature. The results of this statistical analysis demonstrate that features 1 to 15 exhibit a high frequency for each statistical parameter, indicating their significant involvement in the prediction task.

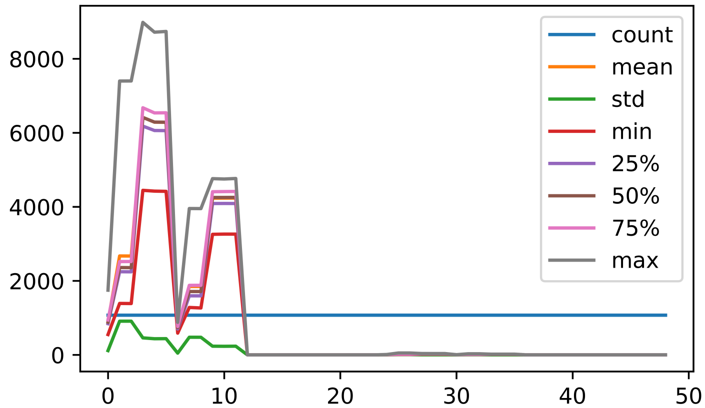

Figure 7: The dataset features statistical analysis.

The pair plot analysis depicted in Figure 8 provides significant insights into the correlations and interdependencies among the four most prominent features selected in the dataset. The analysis employs a grid of scatter plots to visually depict the correlation between each feature and others, as well as the distribution of data points across various target labels. The pair plots reveal a notable degree of scattering, indicating that the chosen features demonstrate substantial variations throughout the dataset and lack strong correlations with one another. This is helpful for developing a ML model because it shows that these features are informative and provide distinctive information for classification. Moreover, the distinct segregation of data points according to distinct target labels serves as a favorable indication for the classification task. This implies the presence of a discernible pattern or arrangement within the data, which can be effectively utilized by a ML model to precisely categorize samples into their corresponding classes.

4. Results and Discussions

The dataset used in the study contained multiple categories, and the distribution of labels within each category is shown in Figure 9. To ensure an unbiased evaluation of the machine learning models, the dataset was divided into training and testing sets using a 70:30 ratio. This means that 70% of the available data was used for training the models, while the remaining 30% was kept aside for evaluating their effectiveness.

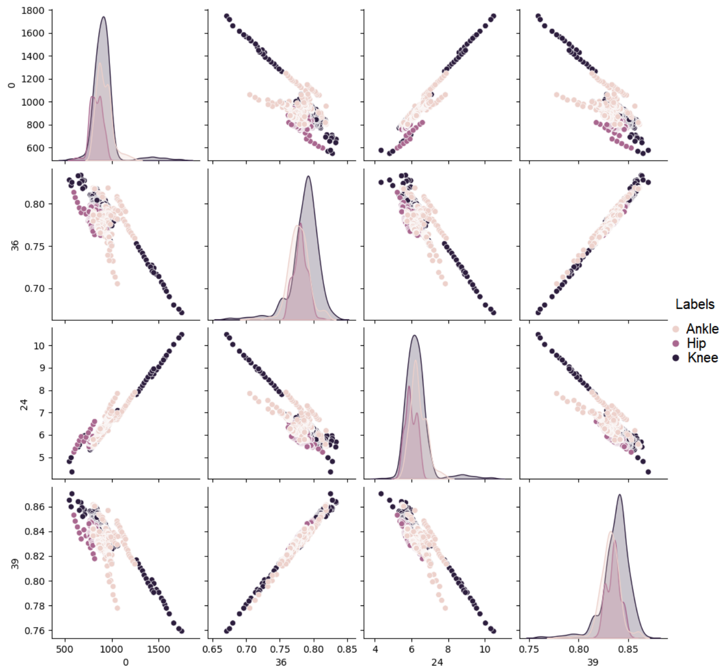

Figure 8: The pair plot analysis of selected top 4 features.

Several traditional ML models were trained with specific hyperparameters selected using grid search are given in Table 2. The selection of these models is based on their comprehensive understanding, extensive research, and demonstrated efficacy in managing medical data across diverse applications.

The Random Forest (RF) model utilized a maximum depth of 300 and 300 estimators. The Decision Tree (DT) model was trained with a maximum depth of 300. The Logistic Regression (LR) model had a random state of 0, a maximum iteration of 1000, and the 'liblinear' solver. The Gaussian Naive Bayes (GNB) model used a variance smoothing value of 2. Additionally, an LSTM model was trained as part of the study. It employed a categorical cross-entropy loss function, the Adam optimizer, and accuracy as the evaluation metric. These hyperparameters were selected using the grid search. The classification results are shown in Table 3 ans visualized in Figure 10.

It is evident from Table 3 and Figure 10 that the RF model exhibited superior performance, attaining accuracy, precision, recall, and F1 score of 0.94, thereby indicating its robust predictive ability and capacity to capture

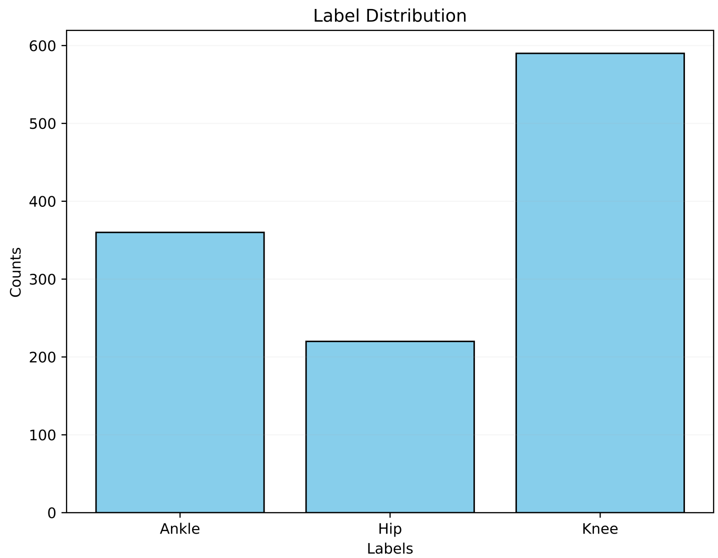

Figure 9: The distribution analysis of dataset along with the target label.

invisible patterns. The DT model exhibited strong performance, achieving scores of 0.86 across all metrics. The LR model demonstrated inferior performance, as indicated by accuracy, precision, recall, and an F1 score of 0.65. The GNB and LSTM models exhibited a performance that was equivalent to chance, as evidenced by their accuracy scores of 0.50.

4.1. Results of k-fold cross validations

K-fold cross-validation is a widely used technique in machine learning to evaluate the performance of a model. This method involves partition-

Table 2: Hyperparameter values for different techniques.

Technique	Hyperparameter Values
RF	`max_depth`=300, `n_estimators`=300
DT	`max_depth`=300
LR	`random_state`=0, `max_iter`=1000, `solver`='liblinear'
GNB	`var_smoothing`=2
LSTM	`loss`='categorical_crossentropy', `optimizer`='adam', `metrics`='accuracy'

Table 3: Performance metrics of different techniques on unseen data

Technique	Accuracy	Precision	Recall	F1 Score
RF	0.94	0.94	0.94	0.94
DT	0.86	0.86	0.86	0.86
LR	0.65	0.65	0.65	0.64
GNB	0.50	0.38	0.50	0.39
LSTM	0.50	0.25	0.50	0.34

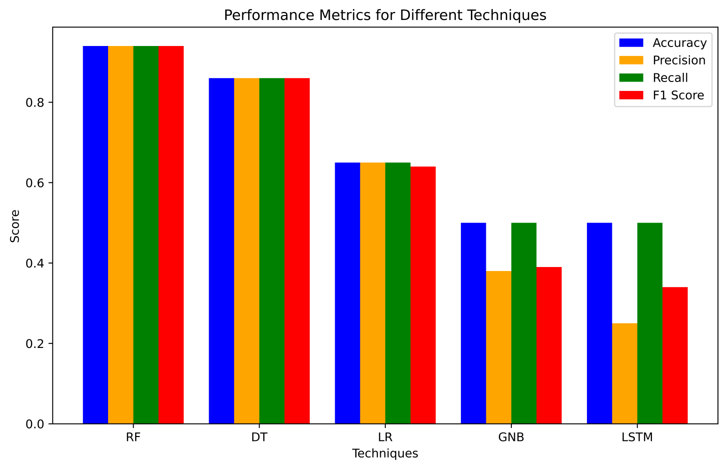

Figure 10: Visualization of result of classifiers on unseen data.

ing the GLCM statistical feature dataset extracted from images into k non-overlapping subsets or folds, where k is a positive integer. The model is then trained on k-1 folds and tested on the remaining fold. This process is repeated k times, with each fold serving as the test set once. The results are then averaged to obtain a more reliable estimate of the model's performance. The model undergoes k-fold cross-validation, where k iterations are performed. In each iteration, one of the k folds is designated as the test set, while the remaining k-1 folds are utilized for training. By adopting this methodology, a more comprehensive assessment can be achieved as it reduces the influence of data partitioning on the efficacy of the model. The accuracy values that were reported offer a mean performance metric across the 10 folds, whereas the standard deviations reflect the extent of diversity in the outcomes. The study employed k-fold cross-validation technique with 10 folds to assess the efficacy of the models. The results are shown in Table 4.

Table 4: Results of K fold validation.

Technique	Accuracy	Standard Deviations (+/-)
RF	0.93	0.0271
DT	0.87	0.0402
LR	0.65	0.0334
GNB	0.49	0.0328
LSTM	0.40	0.4671

It is evident from Table 4 that the RF model achieved the highest accuracy of 0.93 with a low standard deviation of 0.0271, indicating consistent and reliable performance. The DT model had an accuracy of 0.87 and a slightly higher standard deviation of 0.0402, showing stable performance but with a bit more variability. The LR model had an accuracy of 0.65 and a standard deviation of 0.0334, suggesting some sensitivity to different data splits. The GNB model performed the poorest with an accuracy of 0.49 and a standard deviation of 0.0328, indicating both low accuracy and variability. Overall, the RF model demonstrated the highest and most stable performance, while the other models showed varying levels of accuracy and consistency. A bar graph is shown in Figure 11 where the x-axis represents the techniques (RF, DT, LR, GNB), the y-axis represents the accuracy, and the error bars indicate the standard deviations.

4.2. Performance analysis with data balancing

A comprehensive assessment of the performance of various methods when employing the data balancing technique known as Synthetic Minority Oversampling Technique (SMOTE) is provided in Table 5 and visulaized in Figure 12(a) and 12(b). The findings indicate that the performance of the GNB and LSTM methods was poor when the data balancing technique was applied. In contrast, the RF and DT methods exhibited modest enhancements in their performance. Based on the analysis conducted, it can be deduced that the implementation of data balancing techniques does indeed improve the overall performance. However, it is important to note that the effectiveness of these techniques varies across the different methods that were examined in this study. Kfold cross validation results shows that RF and DT have highest average accuracy with a low standard deviation that can be seen in Figure 12.

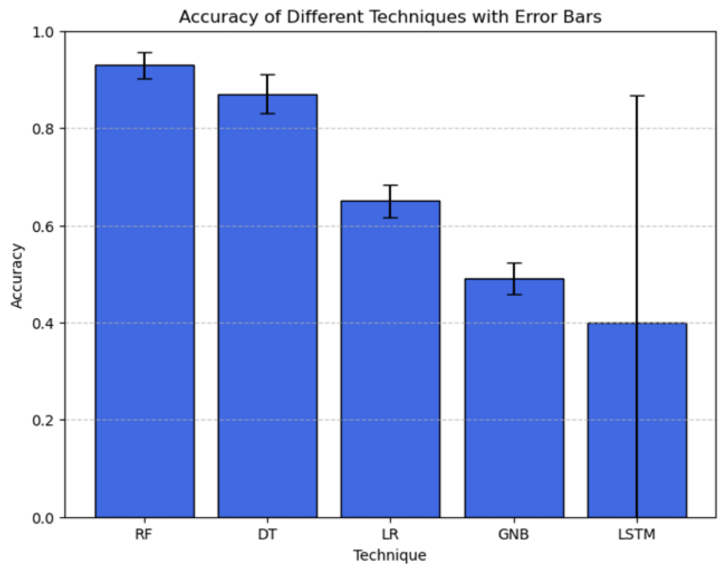

Figure 11: Visualization of cross validation results with error bars.

Table 5: Performance metrics on balanced data with Kfold scores for different techniques

Technique	Accuracy	Precision	Recall	F1 Score	Kfold score with std
RF	0.96	0.96	0.96	0.96	0.964 ± 0.0187
DT	0.91	0.91	0.91	0.91	0.924 ± 0.024
LR	0.69	0.69	0.69	0.69	0.683 ± 0.029
GNB	0.37	0.27	0.37	0.26	0.369 ± 0.024
LSTM	0.32	0.11	0.32	0.16	0.409 ± 0.467

The performance validation of the proposed RF method for male and female patient data was conducted separately. The findings presented in Table 6 and visualized in Figure 13 demonstrate that the model exhibited equivalent scores for male and female patients, suggesting the absence of substantial gender bias. The observed high values of accuracy, precision, recall, and F1 score for both groups provide empirical evidence supporting the fairness and impartiality of the proposed approach in managing gender-related data. The finding holds significant importance in guaranteeing transparency and reliability in the practical implementation of the model, specifically in vital sectors such as healthcare.

4.3. Computational complexity analysis

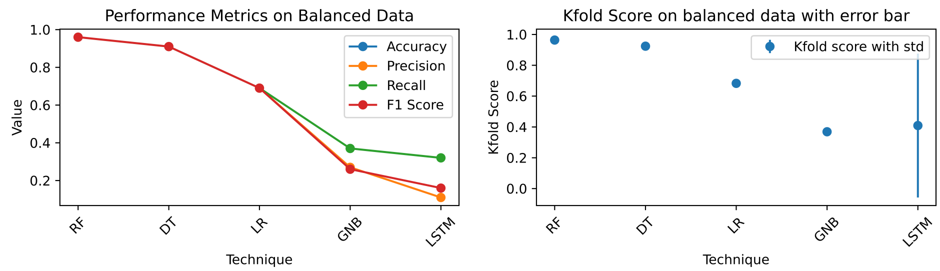

(a)

(b)

Figure 12: (a) Performance metrices on balanced dataset.(b)Cross validation results with error bars.

Table 6: Performance metrics comparison for male and female patients.

Performance Metrics	Results	
	Male Patients	Female Patients
Accuracy	0.96	0.95
Precision	0.96	0.96
Recall	0.96	0.95
F1 Score	0.96	0.95

In addition to the results and discussions on lower limb disorder (Ankle, Knee and Hip) classification using the GLCM statistical features extracted from the mesh images, the research also conducted a computational complexity analysis of various machine learning and deep learning techniques, as presented in Table 7. An open-source platform Google Collab with a GPU backend with 13 GB RAM used during the model's complexity analysis. This analysis provided insights into the runtime computation costs associated with each approach. Among the evaluated techniques, the deep learning-based LSTM model demonstrated the highest runtime computation cost, with a recorded value of 23.98 seconds. This indicates that the LSTM model required significant computational resources for training and inference processes. On the other hand, machine learning techniques such as DT, LR, and GNB achieved relatively lower computation costs. However, it should be noted that these techniques also exhibited lower performance accuracy scores in comparisons. This suggests a trade-off between computational efficiency and classification accuracy. On the other hand, the proposed RF technique achieved a moderate computation score of 1.49 seconds while maintaining

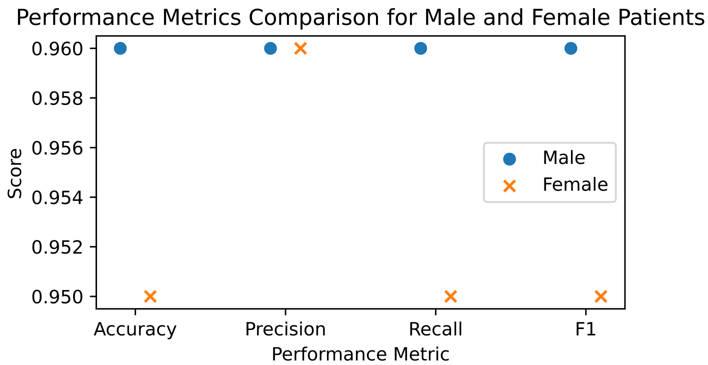

Figure 13: Visualization of performance metrics comparison for male and female patients.

high performance accuracy scores.

Table 7: Runtime computations for different techniques.

Technique	Runtime Computations (Seconds)
RF	1.490
DT	0.184
LR	0.169
GNB	0.011
LSTM	23.98

5. Conclusion

This study presented a comprehensive methodology for gait analysis and injury diagnosis using force-sensing resistor (FSR) sensors. The research demonstrated the potential of FSR sensors in capturing force distribution during walking, offering valuable insights into the biomechanics of human locomotion. By extracting relevant features from the sensor data and employing machine learning models, the study achieved accurate classification of disorders in the hip, knee, and ankle joints. The Random Forest (RF) model exhibited the highest accuracy on the balanced dataset of 96%, highlighting its robust predictive ability. The study emphasized the importance of preprocessing and feature extraction techniques in analyzing the collected data, ensuring the quality and relevance of the extracted features. Furthermore, the use of k-fold cross-validation with 10 folds provided a comprehen-

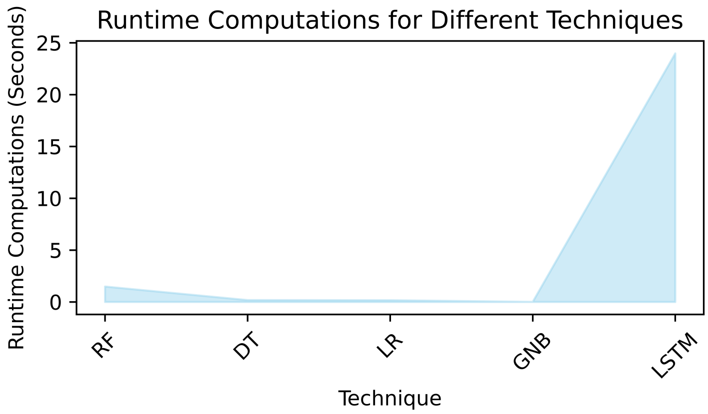

Figure 14: Visualization of time complexity in seconds.

sive evaluation of the models' performance and reduced the impact of data partitioning. Overall, this research contributes to the field of gait analysis and injury diagnosis, showcasing the potential of FSR sensors and machine learning techniques for improving the assessment of lower limb injuries. Future work in this area could focus on several aspects to further enhance the methodology for gait analysis and injury diagnosis using FSR sensors. Firstly, performing comprehensive analysis data and applying deep learning models. Additionally, expanding the scope of the injury classification to include a wider range of lower limb injuries, beyond the hip, knee, and ankle joints, would provide a more comprehensive understanding of the methodology's capabilities.

Institutional Review Board Statement: The study was conducted in accordance with the Declaration of Helsinki and approved by the Institutional Review Board (or Ethics Committee) of KFUEIT.

Informed Consent Statement: Informed consent was obtained from all subjects involved in the study.

Competing Interests: The authors declare no competing interests.

Funding: The authors declare that they received no funding for this research study.

Data Availability: The data used in this study is available upon request.

References

Abdelhady, M., van den Bogert, A.J., Simon, D., 2019. A high-fidelity wearable system for measuring lower-limb kinetics and kinematics. IEEE Sensors Journal 19, 12482–12493.

Abdul Razak, A.H., Zayegh, A., Begg, R.K., Wahab, Y., 2012. Foot plantar pressure measurement system: A review. Sensors 12, 9884–9912.

Arduino, 2018. What is arduino? URL: https://www.arduino.cc/en/Guide/Introduction. accessed on 2 August 2023.

Ben, . What is an arduino? URL: https://learn.sparkfun.com/tutorials/what-is-an-arduino/all. accessed on 2 August 2023.

Brown, R., Ghavami, N., Adjrad, M., Ghavami, M., Dudley, S., 2017. Occupancy based household energy disaggregation using ultra wideband radar and electrical signature profiles. Energy and Buildings 141, 134–141.

Callahan, L.F., Cleveland, R.J., Allen, K.D., Golightly, Y., 2021. Racial/ethnic, socioeconomic, and geographic disparities in the epidemiology of knee and hip osteoarthritis. Rheumatic Disease Clinics 47, 1–20.

Carr, A.J., Robertsson, O., Graves, S., Price, A.J., Arden, N.K., Judge, A., Beard, D.J., 2012. Knee replacement. The Lancet 379, 1331–1340.

Chen, F., Cui, X., Zhao, Z., Zhang, D., Ma, C., Zhang, X., Liao, H., 2020. Gait acquisition and analysis system for osteoarthritis based on hybrid prediction model. Computerized Medical Imaging and Graphics 85, 101782.

Chopra, S., Crevoisier, X., 2019. Preoperative gait asymmetry in end-stage unilateral ankle osteoarthrosis patients. Foot and Ankle Surgery 25, 298–302.

Cueva, J.H., Castillo, D., Espinós-Morató, H., Durán, D., Díaz, P., Lakshminarayanan, V., 2022. Detection and classification of knee osteoarthritis. Diagnostics 12, 2362. URL: https://www.mdpi.com/2075-4418/12/10/2362.

Cui, X., Zhao, Z., Ma, C., Chen, F., Liao, H., . A gait character analyzing system for osteoarthritis pre-diagnosis using rgb-d camera and supervised classifier.

Dell'Isola, A., Pihl, K., Turkiewicz, A., Hughes, V., Zhang, W., Bierma-Zeinstra, S., Prieto-Alhambra, D., Englund, M., 2022. Risk of comorbidities following physician-diagnosed knee or hip osteoarthritis: a register-based cohort study. Arthritis Care & Research 74, 1689–1695.

Devereux, R.B., Pini, R., Aurigemma, G.P., Roman, M.J., 1997. Measurement of left ventricular mass: methodology and expertise. Journal of hypertension 15, 801–809.

Faludi, R., 2010. Building wireless sensor networks: with ZigBee, XBee, arduino, and processing. " O'Reilly Media, Inc.".

Fatima, S.Z., 2022. Life of an amputee: predictors of quality of life after lower limb amputation. Wiener Medizinische Wochenschrift , 1–5.

Ferreira, G.E., McLachlan, A.J., Lin, C.W.C., Zadro, J.R., Abdel-Shaheed, C., O'Keeffe, M., Maher, C.G., 2021. Efficacy and safety of antidepressants for the treatment of back pain and osteoarthritis: systematic review and meta-analysis. Bmj 372.

FSR, . Interface force sensor (fsr) with arduino – measure force. URL: `https://microcontrollerslab.com/force-sensor-fsr-arduino-tutorial/`. accessed on 2 August 2023.

Goldberg, A.J., MacGregor, A., Dawson, J., Singh, D., Cullen, N., Sharp, R.J., Cooke, P.H., 2012. The demand incidence of symptomatic ankle osteoarthritis presenting to foot & ankle surgeons in the united kingdom. The Foot 22, 163–166.

Grimmer, M., Riener, R., Walsh, C.J., Seyfarth, A., 2019. Mobility related physical and functional losses due to aging and disease-a motivation for lower limb exoskeletons. Journal of neuroengineering and rehabilitation 16, 1–21.

Hamza, A., Khan, M.A., Alhaisoni, M., Al Hejaili, A., Shaban, K.A., Alsubai, S., Alasiry, A., Marzougui, M., 2023. D2bof-covidnet: A framework of deep bayesian optimization and fusion-assisted optimal deep features for covid-19 classification using chest x-ray and mri scans. Diagnostics 13, 101.

Heidari, B., 2011. Knee osteoarthritis diagnosis, treatment and associated factors of progression: part ii. Caspian journal of internal medicine 2, 249.

Herrera-Pérez, M., González-Martín, D., Vallejo-Márquez, M., Godoy-Santos, A.L., Valderrabano, V., Tejero, S., 2021. Ankle osteoarthritis aetiology. Journal of clinical medicine 10, 4489.

Herrera-Pérez, M., Valderrabano, V., Godoy-Santos, A.L., de César Netto, C., González-Martín, D., Tejero, S., 2022. Ankle osteoarthritis: comprehensive review and treatment algorithm proposal. EFORT open reviews 7, 448–459.

Hunter, D.J., March, L., Chew, M., 2020. Osteoarthritis in 2020 and beyond: a lancet commission. The Lancet 396, 1711–1712.

Jun, K., Lee, S., Lee, D.W., Kim, M.S., 2021. Deep learning-based multimodal abnormal gait classification using a 3d skeleton and plantar foot pressure. IEEE Access 9, 161576–161589.

Kabir, A.S., Shorif, M.A., Li, H., Yu, Q., 2014. A study of secured wireless sensor networks with xbee and arduino, in: The 2014 2nd International Conference on Systems and Informatics (ICSAI 2014), IEEE. pp. 492–496.

Khalid, H., Hussain, M., Al Ghamdi, M.A., Khalid, T., Khalid, K., Khan, M.A., Fatima, K., Masood, K., Almotiri, S.H., Farooq, M.S., 2020. A comparative systematic literature review on knee bone reports from mri, x-rays and ct scans using deep learning and machine learning methodologies. Diagnostics 10, 518.

Kotti, M., Duffell, L.D., Faisal, A.A., McGregor, A.H., 2017. Detecting knee osteoarthritis and its discriminating parameters using random forests. Medical engineering & physics 43, 19–29.

Kwon, S.B., Han, H.S., Lee, M.C., Kim, H.C., Ku, Y., 2020. Machine learning-based automatic classification of knee osteoarthritis severity using gait data and radiographic images. IEEE Access 8, 120597–120603.

Leggit, J., Mark, R., Hulsopple, C., Carey, P.M., Alisangco, J.B., 2022. Disorders of the Lower Extremity. Springer International Publishing, Cham. URL: https://doi.org/10.1007/978-3-030-54441-6_118, doi:10.1007/978-3-030-54441-6_118.

Li, G., Liu, T., Yi, J., Wang, H., Li, J., Inoue, Y., 2016. The lower limbs kinematics analysis by wearable sensor shoes. IEEE Sensors Journal 16, 2627–2638.

Malvade, P.S., Joshi, A.K., Madhe, S.P., . Iot based monitoring of foot pressure using fsr sensor.

Picerno, P., 2017. 25 years of lower limb joint kinematics by using inertial and magnetic sensors: A review of methodological approaches. Gait & posture 51, 239–246.

Pirani, H., Noori, S., Shahmoradi, D., 2019. Examining the prevalence of lower body disorders among male lower-secondary education students in kermanshah. International Journal of Health and Life Sciences 5.

Rana, N.K., . Application of force sensing resistor (fsr) in design of pressure scanning system for plantar pressure measurement.

Shu, L., Hua, T., Wang, Y., Li, Q., Feng, D.D., Tao, X., 2010. In-shoe plantar pressure measurement and analysis system based on fabric pressure sensing array. IEEE Transactions on information technology in biomedicine 14, 767–775.

Shuzan, M.N.I., Chowdhury, M.E.H., Reaz, M.B.I., Khandakar, A., Abir, F.F., Faisal, M.A.A., Ali, S.H.M., Bakar, A.A.A., Chowdhury, M.H., Mahbub, Z.B., 2023. Machine learning-based classification of healthy and impaired gaits using 3d-grf signals. Biomedical Signal Processing and Control 81, 104448.

Siddiqui, H., 2016. Automated peripheral sensory neuropathy assessment of diabetic patients using optical imaging and binary processing techniques.

Slijepcevic, D., Zeppelzauer, M., Gorgas, A.M., Schwab, C., Schüller, M., Baca, A., Breiteneder, C., Horsak, B., 2017. Automatic classification of functional gait disorders. IEEE journal of biomedical and health informatics 22, 1653–1661.

Valderrabano, V., Horisberger, M., Russell, I., Dougall, H., Hintermann, B., 2009. Etiology of ankle osteoarthritis. Clinical Orthopaedics and Related Research® 467, 1800–1806.

Verlekar, T.T., Soares, L.D., Correia, P.L., 2018. Automatic classification of gait impairments using a markerless 2d video-based system. Sensors 18, 2743.

Vos, T., Flaxman, A.D., Naghavi, M., Lozano, R., Michaud, C., Ezzati, M., Shibuya, K., Salomon, J.A., Abdalla, S., Aboyans, V., 2012. Years lived with disability (ylds) for 1160 sequelae of 289 diseases and injuries 1990–2010: a systematic analysis for the global burden of disease study 2010. The lancet 380, 2163–2196.

Wertsch, J.J., Webster, J.G., Tompkins, W.J., 1992. A portable insole plantar pressure measurement system. J Rehabil Res Dev 29, 13–18.

Weygers, I., Kok, M., Konings, M., Hallez, H., De Vroey, H., Claeys, K., 2020. Inertial sensor-based lower limb joint kinematics: A methodological systematic review. Sensors 20, 673.

Xbee, D., . Digi xbee 802.15.4 protocol comparison. URL: `https://www.digi.com/resources/library/technical-briefs/xbee-802-15-4-protocol-comparison`. accessed on 2 August 2023.

Zeng, W., Ma, L., Zhang, Y., 2023. Detection of knee osteoarthritis based on recurrence quantification analysis, fuzzy entropy and shallow classifiers. Multimedia Tools and Applications , 1–22.